AGENCY FOR INTERNATIONAL DEVELOPMENT
WASHINGTON, D. C. 20523

BIBLIOGRAPHIC INPUT SHEET

FOR AID USE ONLY

1. SUBJECT CLASSIFICATION
A. PRIMARY: Agriculture
B. SECONDARY: Irrigation

2. TITLE AND SUBTITLE
Flow through vortex tube sediment ejectors

3. AUTHOR(S)
Mahmood,Khalid

4. DOCUMENT DATE	5. NUMBER OF PAGES	6. ARC NUMBER
1975	30p.	ARC

7. REFERENCE ORGANIZATION NAME AND ADDRESS
Engineering Research Center, Colorado State University, Fort Collins, Colorado 80521

8. SUPPLEMENTARY NOTES (Sponsoring Organization, Publishers, Availability)
(In ASCE Irrigation and Drainage Div. Specialty Conf., Logan, Utah. Proc.p.421-450)

9. ABSTRACT
An analytical model of the flow and sediment conduction through a vortex tube has been developed herein. This model combines the spatially varied flow equations with the sediment transport model in sand bed channels. The empirical coefficients introduced in the model have been investigated with the help of Robinson's 8-ft. flume data (10). It is found that the coefficients of velocity C_v, of area C_a and of lateral momentum inflow C_{IL} can be considered as constants for the tubes investigated by Robinson. However, the vortex flow coefficient, C_I is found to be a function of the tube geomtry and the Froude numver of flow on the tube. Knowing the C_I - IF relation for a specific tube geometry, it is possible to use this model to investigate various characteristics of the vortex tube flow. Three numerical examples have been used to show the verification of laboratory study data, and the effect of variation of parameters on the sediment conduction through the tube.

10. CONTROL NUMBER	11. PRICE OF DOCUMENT
PN-AAB-308	

12. DESCRIPTORS
Channel flow
Hilsch tubes
Models
Sediment transport

13. PROJECT NUMBER
931-11-120-115

14. CONTRACT NUMBER
CSD-2460 211(d)

15. TYPE OF DOCUMENT

FLOW THROUGH VORTEX TUBE SEDIMENT EJECTORS

Abstract

An analytical model of the flow and sediment conduction through a vortex tube has been developed herein. This model combines the spatially varied flow equations with the sediment transport model in sand bed channels. The empirical coefficients introduced in the model have been investigated with the help of Robinson's 8-ft. flume data (10). It is found that the coefficients of velocity C_v, of area C_a and of lateral momentum inflow C_{IL} can be considered as constants for the tubes investigated by Robinson. However, the vortex flow coefficient, C_I is found to be a function of the tube geomtry and the Froude number of flow on the tube. Knowing the C_I - IF relation for a specific tube geometry, it is possible to use this model to investigate various characteristics of the vortex tube flow. Three numerical examples have been used to show the verification of laboratory study data, and the effect of variation of parameters on the sediment conduction through the tube.

Reprinted from the Proceedings of the ASCE Irrigation and Drainage Division Specialty Conference held at Logan, Utah August 13-15, 1975.

FLOW THROUGH VORTEX TUBE SEDIMENT EJECTORS

by
Khalid Mahmood[1], M.ASCE

In the design of irrigation diversion and distribution systems supplied from alluvial rivers, a major consideration is the sediment discharge equilibrium of the system. Generally it is more economical to control the sediment inflow at the diversion structures and to eject excess sediment near the headworks than to treat a sediment problem that has been diffused through the distribution system. Therefore, under the usual conditions encountered in diversions from sand bed rivers, sediment discharge equilibrium can be optimally achieved by limiting the sediment discharge past the head reaches to the sediment handling capacity of the system.

A variety of sediment control measures have been evolved in the past. Of the on-line, continuous-operation sediment control measures, the vortex tube ranks as the more successful structure. A vortex tube sediment ejector consists of a tube built in the crest of a bed contraction. The tube has a longitudinal slit on top and is laid across the flow normally or at an angle of 30° to 90°. The tube discharges into an escape channel and the discharge end of the tube can be under free or submerged flow condition. The schematic layout of a vortex tube sediment ejector is shown in Figure 1.

The hydraulic and sediment conduction characteristics of vortex tubes have been investigated in a number of studies (1,3,5,9,10,11). Most of these studies have been laboratory scale model studies. These studies served a useful purpose at the time in explaining the behavior and action of vortex tubes and in developing their design criteria. However, the water and sediment conduction through the vortex tube involves two distinct phenomena: (1) the spatially varied flow in the tube and (2) the sediment transport as bed load and as suspended load in the approach flow. It is nearly impossible to simultaneously scale relevant aspects of these two phenomena in small scale physical model studies. The laboratory studies are therefore of a limited value when their results are to be extrapolated to different size scales or to different sediment transport regimes. To overcome this difficulty, an analytical model is developed herein for the hydraulic and sediment conduction aspects of vortex tubes. The verification of this model and the evaluation of empirical coefficients have been made from Robinson's data on nine different vortex tubes studied by him in an 8 ft flume at Colorado State University (10). The use of this model is also illustrated for the study of various design and sediment conduction characteristics of vortex tube flow

[1]Associate Professor, Civil Engineering Department, Colorado State University, Fort Collins, Colorado 80523

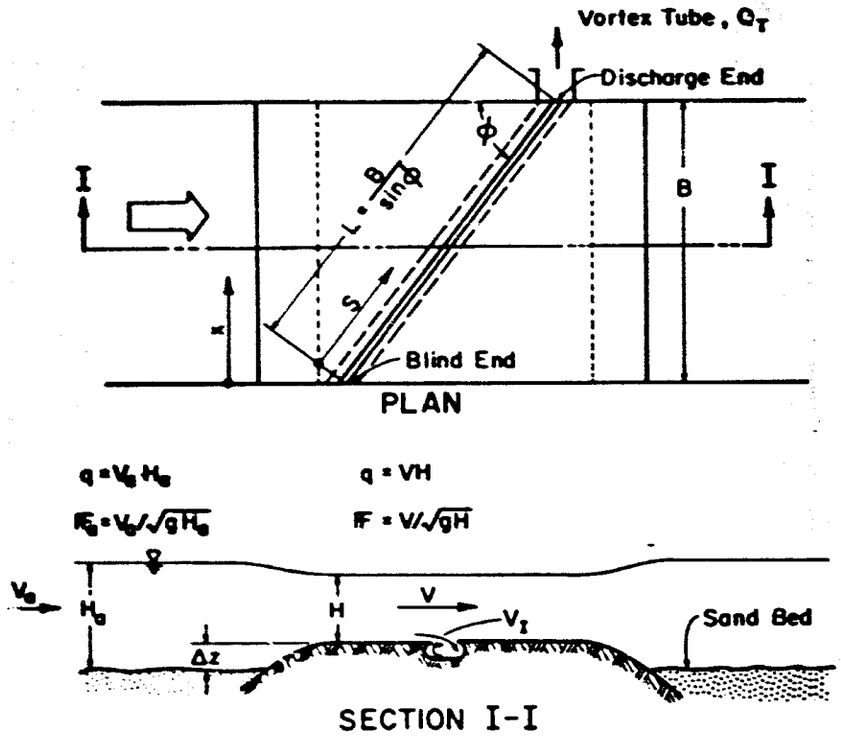

Figure 1. Schematic Layout of a Vortex Tube.

HYDRAULICS OF A VORTEX TUBE

Hydraulically, there are two characteristics of the vortex tube flow: (1) the flow is spatially varied along the length of the tube and (2) a vortex is superimposed on the longitudinal flow due to the flow entering the tube. To analyze the flow through the tube, the force-momentum relations are applied as follows:

Equations of Flow

Consider a cross-section of the vortex tube normal to its length (Figure 2). At this section, one dimensional continuity and momentum equations can be written along coordinate s measured along the centerline of the tube as:

$$\frac{dQ}{ds} = q_I = C_a\, a\, C_v\, \sqrt{2g\ \Delta h_e} = C_a\, a\, V_I \qquad (1)$$

and

$$\frac{dF}{ds} = \frac{d}{ds}\left(\rho\, \frac{Q^2}{A}\right) - C_{IL}\, \rho\, q_I V_I \cos\phi \qquad (2)$$

where Q = longitudinal discharge in the tube, q_I = inflow discharge intensity per unit length of the tube, $(C_a\, a)$ = effective area of the slit per unit length of the tube, normal to the velocity of inflow (V_I), F = sum of all the forces acting on this cross-section along s direction; ρ = mass density of the fluid, A = cross sectional area of the tube normal to its length and C_{IL} = coefficient of lateral momentum inflow in the tube due to q_I. In Equations (1) and (2), quantities, q_I, a, V_I, F, Q and A are functions of coordinates. However the coefficients C_a, C_v and C_{IL} are considered independent of s and entirely dependent on the tube geometry. Their evaluation will be discussed later.

Vortex Flow

Based on the descriptions of the flow in the laboratory and prototype vortex tube structures (5,9,10,11), it is known that at the cross-section under consideration, a forced vortex, is generated due to the inflow. It is assumed that the vortex has an angular velocity, ω (a function of s) and that the tangential velocity V_c at the periphery of the tube is related to the inflow velocity component normal to the tube axis, $V_I \sin\phi$ (Figure 2) as

$$V_c = \frac{\omega d}{2} = C_I V_I \sin\phi = \frac{C_I q_I}{C_a a} \sin\phi \qquad (3)$$

where d = depth of tube invert below its upstream lip (Figure 3) and the vortex flow coefficient C_I depends on geometry and layout parameters of the tube as well as on the velocity and velocity distribution of the approach flow. It is assumed that $C_I > 0$ even when the downstream lip of the tube is at or below the level of the upstream lip ($e \leq 0$ in Figure 3).

Pressure Distribution in the Flow

To resolve the pressure distribution in the cross-section, it is assumed that the flow can be decomposed in a nearly parallel flow along the length of the tube and the forced vortex as described above.

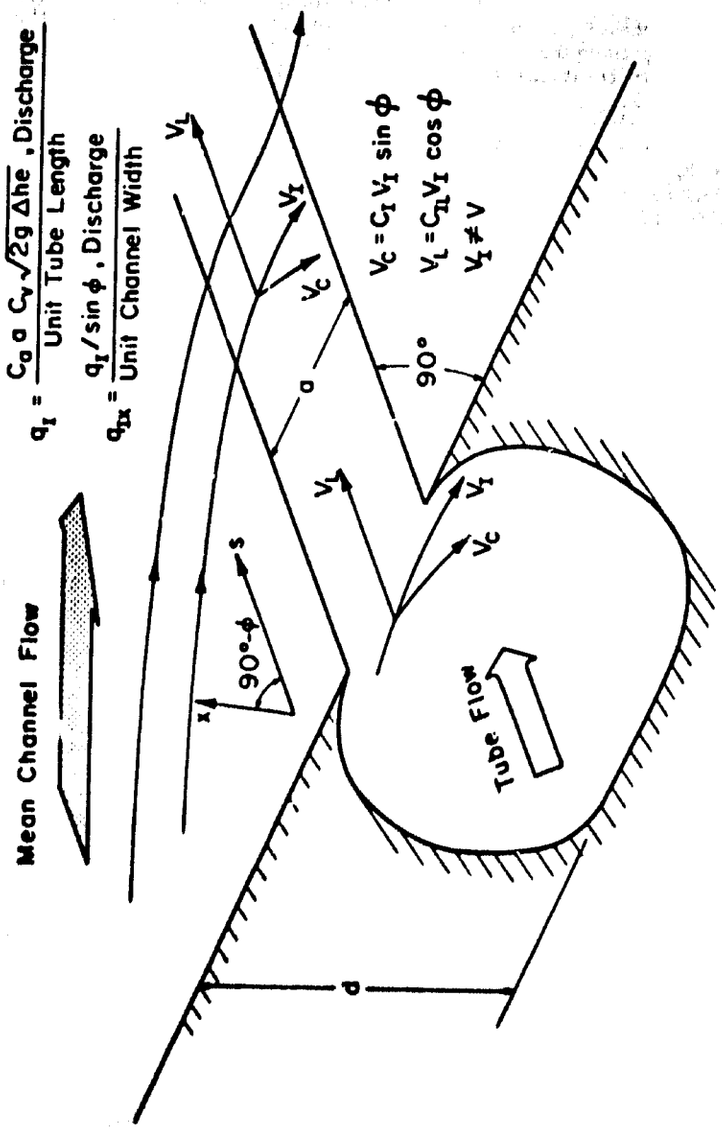

Figure 2. Inflow Velocity Components in an Inclined Vortex Tube.

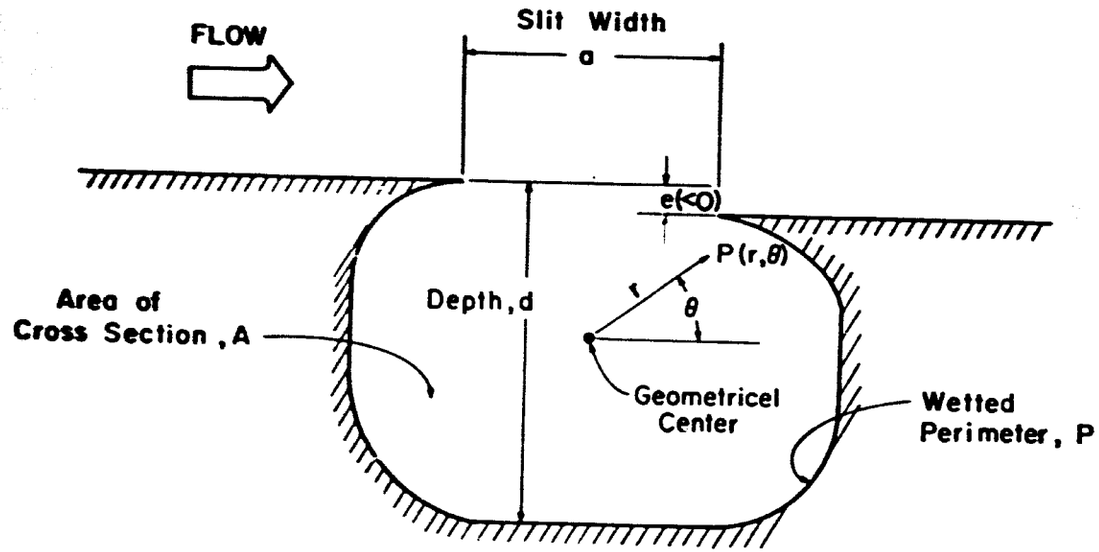

Figure 3. Geometrical Parameters of Vortex Tube on a Cross Section Normal to Tube Length.

The pressure distribution is then obtained by the superposition of: (1) hydrostatically varying pressure along the depth of the tube and (2) the pressure field due to the vortex. Considering a point (r,θ) in the cross-section, Figure 3,

$$p(r,\theta) = p_c - \rho g r \sin\theta + \frac{2\rho q_I^2 C_I^2 \sin^2\phi}{C_a^2 a^2} \left(\frac{r}{d}\right)^2 \tag{4}$$

where p_c = pressure on the centerline of the tube $(r=0)$ and g = gravitational acceleration. At the top of the tube, in the plane of the slit,

$$P_I = p\left(\frac{d}{2}, \frac{\pi}{2}\right) = p_c - \rho g \frac{d}{2} + \rho \frac{q_I^2 C_I^2 \sin^2\phi}{2 C_a^2 a^2} \tag{5}$$

and the average pressure on the cross-section is

$$\bar{p} = p_c + \frac{\rho}{4} \frac{q_I^2 C_I^2 \sin^2\phi}{C_a^2 a^2} \tag{6}$$

Inflow Discharge Intensity

The inflow discharge intensity, q_I can be related to the pressure difference across the slit as

$$q_I = C_v C_a a \sqrt{2g\,\Delta he} \tag{7}$$

where C_v = coefficient of velocity and $\Delta he = H - \frac{P_I}{\rho g}$. Equations (7) and (5) can be combined to obtain

$$q_I = A_2 \sqrt{\Delta h} \tag{8}$$

where

$$A_2 = \sqrt{2g\left(\frac{C_v^2 C_a^2 a^2}{1+C_v^2 C_I^2 \sin^2\phi}\right)} \tag{9}$$

and

$$\Delta h = \left(H + \frac{d}{2} - \frac{P_c}{\rho g}\right) \tag{10}$$

Forces Acting on the Cross-Section

Considering all the forces acting on the cross-section

$$\frac{dF}{ds} = \rho g A \sin\alpha - \tau P - \frac{d}{ds}(\bar{p}A) \tag{11}$$

Component due to: gravity-boundary shear-pressure

where α = inclination of the tube invert with the horizontal considered positive downward in the direction of tube flow, τ = boundary shear stress $\frac{\rho f Q^2}{8A^2}$, f = Darcy-Weisbach friction factor, P = wetted perimeter of the tube and A = the cross-sectional area of the tube.

Equation of Flow

Introducing Equation (11) and the expressions for other quantities in Equation (2), yields

$$Q'Q'' + A_*Q'^2 + B_*Q\,Q' + C_*Q^2 + D_* = 0 \qquad (12)$$

where

$$Q' = \frac{dQ}{ds},\ Q'' = \frac{dQ'}{ds},\ A_* = \frac{1}{2A}\frac{dA}{dS} - \frac{1}{a}\frac{da}{ds} + \frac{2aC_{IL}\cos\phi}{C_a A A_1},\ B_* = -\frac{4a^2}{A^2A_1},$$

$$C_* = \frac{-2a^2}{A^3A_1}\left(\frac{fP}{8} - \frac{dA}{ds}\right),\ D_* = \left\{\frac{-2a^2}{A A_1}\,g\,\left(H + \frac{d}{2}\right)\frac{dA}{ds} + \frac{2a^2}{A_1}\,g\sin\alpha\right\}$$

and

$$A_1 = \frac{2 + (C_vC_I\sin\phi)^2}{(C_vC_a)^2}$$

Equation (12) is a second order non-linear differential equation with variable coefficients. The solution of this equation describes the flow and pressure variation along the length of the tube. The manner in which this equation is usually solved makes it a boundary value problem. It can be numerically solved if two boundary conditions are specified. However, in some particular cases, this equation can be analytically solved. The case of a horizontal laid prismatic tube is one such case. The rest of this paper is exclusively concerned with the water and sediment flow through horizontal prismatic tubes.

Solution for Horizontal Prismatic Vortex Tubes

Equation (12) is considerably simplified for the case of a horizontally laid, prismatic tube, that has a constant slit width. For this condition, $D_* = 0$ and Equation (12) becomes a homogeneous equation with constant coefficients:

$$Q'Q'' + A_*Q'^2 + B_*\,Q\,Q' + C_*Q^2 = 0 \qquad (13)$$

The boundary conditions for Equation (13) are

$$Q(0) = 0 \quad \text{and} \quad Q(L) = Q_T$$

where Q_T = discharge at the exit of the vortex tube. Assuming as a solution

$$Q(s) = Q_0 \exp(ks) \qquad (14)$$

where Q_0 = a constant greater than 0, Equation (13) becomes

$$Q_0 \exp[2ks] \cdot \{k^3 + A_*k^2 + B_*k + C_*\} = 0\ . \qquad (15)$$

For a nontrivial solution of Equation (15),

$$k^3 + A_*k^2 + B_*k + C_* = 0. \qquad (16)$$

To be compatible with the physical situation, the largest positive root of Equation (16) substituted in Equation (14) will provide a solution of Equation (13) along the length of the tube. This solution can also satisfy the downstream boundary condition $Q(L) = Q_T$, so

that from Equation (14), $Q_0 = Q_T \exp(-kL)$. However, it can only satisfy the upstream boundary condition asymptotically because $Q(0) \to 0$ as $L \to \infty$ and the tube is not infinitely long. Assuming a long tube so that $Q(0) = Q_T \exp(-kL) \approx 0$, the solution for the discharge in the vortex tube is:

$$Q(s) = Q_T \exp[k(s-L)] \quad . \tag{17}$$

For this solution, the variation of hydraulic quantities in the tube can be obtained as:

Inflow discharge intensity, $q_I = Q_T k \exp[k(s-L)]$ (18)

Differential pressure head from Equation (1),

$$\Delta h = (H + d/2 - p_c/\rho g)$$

and from Equation (18),

$$\Delta h = \frac{Q_T^2 k^2}{A_2^2} \exp[2k(s-L)] \quad . \tag{19}$$

Centerline pressure in the tube, $\frac{p_c}{\rho g} = (H + \frac{d}{2}) - \frac{Q_T^2 k^2}{A_2^2} \exp[2k(s-L)]$ (20)

and,

$$\text{Angular velocity, } \omega = \frac{2Q_T k C_I \sin\phi}{C_a\, a\, d} \exp[k(s-L)] \quad . \tag{21}$$

Equations (17) through (21) indicate that the flow parameters vary exponentially along the length of the tube. The exponential parameter k is determined from Equation (16). It is a function of the tube geometry and the coefficients C_v, C_a, C_I and C_{IL} introduced at various stages of the model. Given the tube geometry and the appropriate values of these coefficients, a unique value of k can be determined.

Evaluation of Coefficients

Coefficients C_v, C_a, C_I and C_{IL} can be indirectly measured by investigating various components of the flow through vortex tubes. In general hydraulic quantities available from the previous vortex tube studies (refer Fig. 1) are the discharge intensity q in the channel, the depth of flow H over the tube, the tube discharge Q_T and the centerline pressure p_{c_e} at the discharge end. In the study reported herein, the writer has used Robinson's data from his 9 experimental series (10) for evaluation of these coefficients. Essentially Robinson, investigated different vortex tube shapes and sizes over a sand bed with the median size, $D_{50} = 0.54$ mm and the gradation coefficient, $\sigma = 2.0$ in an 8 ft recirculating flume. His experimental procedure is described elsewhere (10). All these tubes were placed at $\phi = 45°$ and a wide range of F was investigated for each vortex tube. The data are listed in Table 1. In analyzing Robinson's data, the writer assumed the following values based on his own experience with similar situations in spatially varied flow:

$$C_A = 0.60$$
$$C_v = 0.985$$
$$C_{IL} = 1.00$$

TABLE 1. ROBINSON'S VORTEX TUBE DATA IN 8 FT FLUME.

Run	Flume Discharge Q_{cfs}	Flow on the Tube: Froude No. F	Flow on the Tube: Depth of Flow H_{ft}	Tube Discharge $Q_{T_{cfs}}$	Working head at discharge end $\Delta h(L)$ ft	Vortex coefficient [Eq. (16) & (19)] C_1	Bed Material Concentration: Flume flow (upstream of tube) $C_{C_{ppm}}$	Bed Material Concentration: Tube Flow $C_{T_{ppm}}$
Tube ARR-01, A = 0.244 ft², d = 0.417 ft, P = 1.330 ft, a = 0.625 ft, e = +0.062 ft.								
ARR-01-12	3.95	0.481	0.320	0.920	0.528	2.621	-	-
ARR-01-13	4.75	0.714	0.278	0.872	0.486	2.760	-	-
ARR-01-14	5.16	1.051	0.227	0.785	0.436	3.478	-	-
ARR-01-15	6.99	0.875	0.314	0.935	0.516	2.393	-	-
ARR-01-16	7.23	1.314	0.245	0.835	0.454	2.862	-	-
ARR-01-17	5.34	0.410	0.435	1.030	0.644	2.466	-	-
ARR-01-18	7.30	0.538	0.447	1.060	0.656	2.278	-	-
ARR-01-19	8.50	0.693	0.418	1.050	0.626	2.160	-	-
ARR-01-20	7.45	0.786	0.352	0.975	0.560	2.327	-	-
ARR-01-21	7.79	1.197	0.274	0.935	0.482	2.038	-	-
ARR-01-22	8.15	1.378	0.257	0.775	0.466	4.507	-	-
ARR-01-22b	5.68	0.340	0.514	1.200	0.722	1.685	195	522
ARR-01-23	6.56	0.309	0.603	1.260	0.812	1.749	39	101
ARR-01-24	7.12	0.354	0.581	1.270	0.790	1.602	207	834
ARR-01-25	4.55	0.536	0.327	1.090	0.536	1.343	185	619
Tube ARR-02, A = 0.261 ft², d = 0.417 ft, P = 1.460, a = 0.561 ft, e = +0.005 ft.								
ARR-02-27	7.46	0.852	0.334	1.080	0.542	1.900	821	1477
ARR-02-28	7.57	1.096	0.285	1.020	0.494	1.967	1415	3950
ARR-02-29	6.98	0.431	0.503	1.200	0.712	2.143	226	406
ARR-02-30	7.38	0.490	0.479	1.180	0.688	2.140	617	1450
Tube ARR-03, A = 0.280 ft², d = 0.417 ft, P = 1.590 ft, a = 0.520 ft, e = +0.064 ft.								
ARR-03-31	6.00	0.401	0.477	1.150	0.686	3.216	227	631
ARR-03-32	7.02	0.499	0.458	1.170	0.666	2.788	194	672
ARR-03-33	7.41	0.548	0.446	1.130	0.654	3.132	582	1535
ARR-03-34	7.55	0.713	0.379	1.100	0.588	2.772	831	2960
ARR-03-35	5.68	0.310	0.546	1.230	0.754	2.941	46	117
ARR-03-36	7.54	0.716	0.377	1.150	0.586	2.285	594	1720
Tube ARR-04, A = 0.170 ft², d = 0.440 ft, P = 1.110 ft, a = 0.375 ft, e = -0.062 ft.								
ARR-04-37	5.44	0.422	0.432	0.770	0.652	1.915	181	987
ARR-04-38	6.53	0.582	0.394	0.802	0.614	1.434	482	1550
ARR-04-39	7.38	1.010	0.296	0.714	0.516	1.621	1044	4190
ARR-04-40	7.42	1.165	0.270	0.686	0.490	1.717	1142	5940
ARR-04-41	7.20	0.696	0.373	0.756	0.593	1.705	1088	5400
ARR-04-42	7.10	0.676	0.377	0.777	0.597	1.545	826	3350

TABLE 1 (CONTINUED)

Run	Flume Discharge Q_f cfs	Flow on the Tube: Froude No. F	Flow on the Tube: Depth of Flow H_t ft	Tube Discharge Q_T cfs	Working head at discharge end $\Delta h(L)$ ft	Vortex coefficient [Eq. (16) & (19)] C_I	Bed Material Concentration: Flume flow (upstream of tube) C_f ppm	Bed Material Concentration: Tube flow C_T ppm
Tube ARR-05, A = 0.184 ft^2, d = 0.440 ft, P = 1.240 ft, a = 0.308 ft, e = +0.020 ft.								
ARR-05-43	5.14	0.328	0.492	0.780	0.712	3.050	56	97
ARR-05-44	5.94	0.455	0.436	0.756	0.656	2.918	327	1065
ARR-05-45	6.85	0.597	0.400	0.764	0.620	2.468	858	3610
ARR-05-46	7.27	0.751	0.357	0.644	0.577	4.947	864	5730
ARR-05-47	7.60	0.875	0.332	0.654	0.552	2.509	905	4470
ARR-05-48	7.18	0.992	0.294	0.640	0.514	3.621	740	4050
Tube ARR-06, A = 0.197 ft^2, d = 0.440 ft, P = 1.350 ft, a = 0.287 ft, e = +0.091 ft.								
ARR-06-49	5.59	0.325	0.525	0.820	0.745	3.761	67	123
ARR-06-50	6.74	0.440	0.486	0.817	0.706	3.335	284	8[illegible]
ARR-06-51	6.95	0.607	0.399	0.800	0.619	2.716	924	5790
ARR-06-52	7.26	0.669	0.387	0.867	0.607	1.878	789	3860
Tube ARR-07, A = 0.170 ft^2, d = 0.440 ft, P = 1.110 ft, a = 0.375 ft, e = -0.062 ft.								
ARR-07-52a	18.94	0.622	0.768	1.070	0.988	1.133	1096	3660
ARR-07-53	18.72	0.630	0.756	1.050	0.976	1.207	1911	18317
ARR-07-54	14.72	0.357	0.940	1.130	1.160	1.283	615	3105
ARR-07-55	21.11	1.178	0.540	1.030	0.760	0.566	2067	14453
ARR-07-56	21.23	1.054	0.583	1.040	0.803	0.669	1880	11552
ARR-07-57	20.79	0.829	0.675	1.040	0.895	1.012	1898	11565
ARR-07-58	21.68	1.321	0.509	0.770	0.729	2.363	2062	13769
ARR-07-59	18.65	1.311	0.463	0.700	0.683	3.100	2536	25382
ARR-07-60	18.41	1.181	0.492	0.700	0.712	3.401	1337	9615
ARR-07-61	20.84	1.340	0.491	0.770	0.711	2.249	2915	18662
ARR-07-62	12.05	0.307	0.911	1.110	1.131	1.314	202	278
ARR-07-63	16.47	0.424	0.905	1.170	1.125	0.992	648	4394
ARR-07-64	20.56	0.835	0.667	1.060	0.887	0.875	2188	13699
ARR-07-65	18.89	0.675	0.727	1.080	0.947	0.957	2036	18433
ARR-07-65a	18.85	0.769	0.665	1.050	0.885	0.924	2635	24366
ARR-07-66	18.87	0.705	0.705	1.080	0.925	0.888	2133	15758
ARR-07-67	18.92	0.999	0.560	1.040	0.780	0.590	1651	9462

TABLE 1 (CONTINUED)

RUN	Flume Discharge Q_c cfs	Flow on the Tube: Froude No. F	Flow on the Tube: Depth of Flow H_{ft}	Tube Discharge Q_T cfs	Working head at discharge end $\Delta h(L)$ ft	Vortex coefficient [Eq. (16) & (19)] C_I	Bed Material Concentration: Flume flow (upstream of tube) C_C ppm	Bed Material Concentration: Tube Flow C_T ppm
Tube ARR-08, A = 0.182 ft^2, d = 0.440 ft, P = 1.220 ft, a = 0.325 ft, e = +0.009 ft.								
ARR-08-68	18.84	0.403	1.023	1.190	1.243	1.607	806	2067
ARR-08-69	18.85	0.414	1.005	1.170	1.225	1.671	588	2593
ARR-08-70	21.39	0.532	0.925	1.150	1.145	1.561	740	3329
ARR-08-71	21.29	0.636	0.818	1.120	1.038	1.418	1255	11506
ARR-08-72	19.12	0.713	0.706	1.050	0.926	1.465	1447	7394
ARR-08-73	19.03	0.689	0.720	1.080	0.940	1.338	1142	8455
ARR-08-74	18.74	0.842	0.623	1.030	0.843	1.296	2151	23982
ARR-08-75	18.85	1.086	0.528	0.940	0.74[illegible]	1.489	2679	31221
ARR-08-76	19.32	1.129	0.523	0.980	0.743	1.217	1993	24097
ARR-08-77	17.17	0.845	0.587	1.010	0.807	1.282	1772	13862
ARR-08-78	17.00	1.036	0.509	0.930	0.729	1.476	1641	11714
ARR-08-79	17.27	1.085	0.499	0.970	0.719	1.181	1784	20344
ARR-08-80	17.72	1.015	0.530	1.000	0.750	1.127	2840	25303
ARR-08-81	16.51	0.485	0.827	1.110	1.047	1.501	858	4403
ARR-08-82	16.37	0.692	0.649	1.030	0.869	1.387	1256	7150
Tube ARR-09, A = 0.194 ft^2, d = 0.440 ft, P = 1.330 ft, a = 0.232 ft, e = +0.080 ft.								
ARR-09-84	17.90	0.375	1.037	1.150	1.257	2.465	568	2846
ARR-09-85	19.11	0.464	0.939	1.140	1.159	2.164	742	3279
ARR-09-86	21.12	0.533	0.916	1.160	1.136	1.939	1171	2565
ARR-09-87	21.32	0.687	0.778	1.110	0.998	1.785	1915	15612
ARR-09-88	18.73	0.520	0.859	1.100	1.079	2.164	936	3614
ARR-09-89	18.41	0.606	0.766	1.090	0.986	1.874	1365	12611
ARR-09-90	18.65	0.651	0.738	1.050	0.958	2.054	923	7823
ARR-09-91	19.51	0.845	0.639	1.050	0.859	1.650	1649	17383
ARR-09-92	18.64	0.897	0.595	1.040	0.815	1.540	2257	25727
ARR-09-93	17.81	0.813	0.617	1.030	0.837	1.693	1092	10570

Note: 1 ft = 0.305 m
1 ft^2 = 0.093 m^2
1 cfs = 0.028 m^3/sec.

Admittedly, specific investigations made to evaluate these coefficients may lead to somewhat different values. It is assumed that the vortex flow coefficient, C_I is the only variable that changes with the channel flow. For each run, the value of C_I was computed by trial and error, using the cubic Equation (16) and Equation (19) evaluated at the discharge end (s=L) for $p_{c_e} = 0$. For each tube these values are plotted in Figure 4(a) through (i). To explain the scatter in the calculated C_I - F relationship, the sensitivity of calculated C_I to errors in measurement of Q_T and H was investigated. It was found that:

(1) A change of ± 2 percent in Q_T caused a change of ± 9 percent in the calculated value of C_I.
(2) A change of ± 2 percent in H caused a change of ± 3 percent in the calculated value of C_I.

The maximum probable error in the computed value of C_I due to about 5 percent measurement error in both Q_T and H amounts to about 23 percent. The mean curves drawn for different tube configurations should be viewed in this light. However, these figures do indicate that C_I depends on F. The C_I - F relationships are different for different tube shapes and the mean curves for Robinson's tubes shown in Figure 4 are taken as the characteristic values of individual tube shapes. A combined plot of these mean curves is shown in Figure 5.

Approximate Solution for k and C_I

The preceding analysis of Robinson's data was made by a trial and error solution of Equations (16) and (19). It is also possible to obtain an approximate solution of these equations. Comparing the magnitudes of A_*, B_*, and C_* in Equation (16), one finds that for the usual values of f(≈0.016), C_* is almost negligible as compared to A_* and B_*. Neglecting C_* in comparison with A_* and B_*, Equation (16) is reduced to a quadratic form with a non-negative real root.

$$k = \frac{a}{A}\frac{C_{IL}\cos\phi}{C_a A_1}\left\{\sqrt{1 + \frac{4A_1 C_a^2}{C_{IL}^2\cos^2\phi}} - 1\right\}, \tag{22}$$

As a further approximation

$$k \simeq \frac{2a}{AA_1^{1/2}} = \frac{2aC_vC_a}{A\sqrt{2 + C_v^2C_I^2\sin^2\phi}} \tag{23}$$

and for the values of C_v, C_a and C_{IL} used herein,

$$k \simeq \frac{0.836\ a}{A\sqrt{1 + 0.485\ C_I^2\sin^2\phi}} \tag{24}$$

The preceding model can be used to analyze the flow through a vortex tube, provided the tube geometry, the Froude number of the flow on the tube, the depth of flow H, the centerline pressure at exit p_{ce} and the F - C_I relation for the tube is known. This analysis can be based on the direct solution of Equations (16) and (19). This method is later illustrated herein.

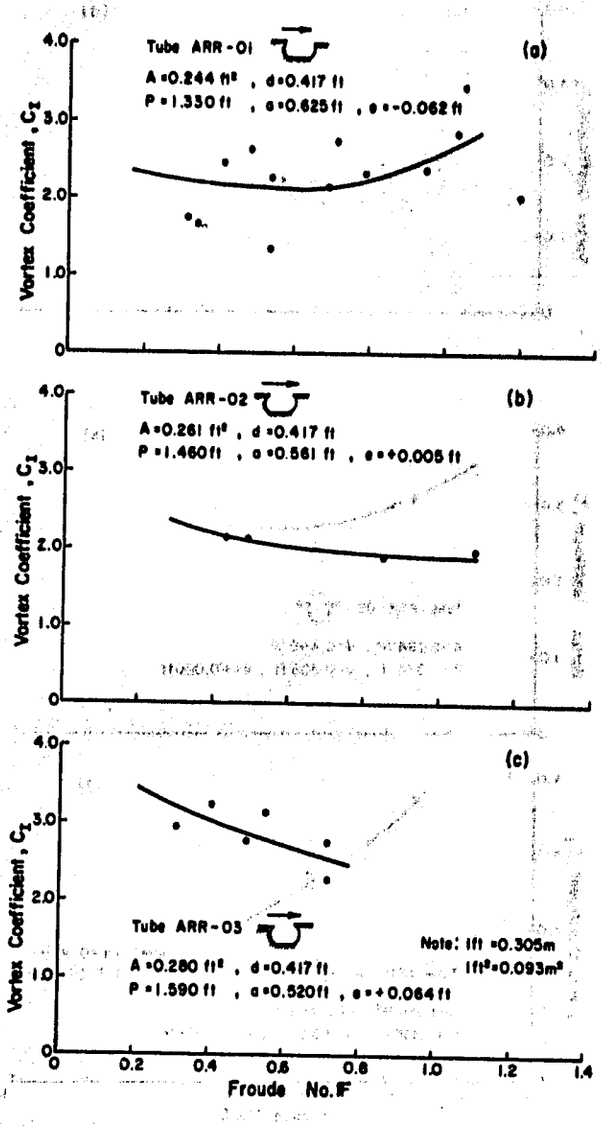

Figure 4(a) - 4(c). Variation of Vortex Coefficient C_I with Froude No. IF in Robinson's Vortex Tubes. In all Tubes, B = 8.0 ft and $\phi = 45°$.

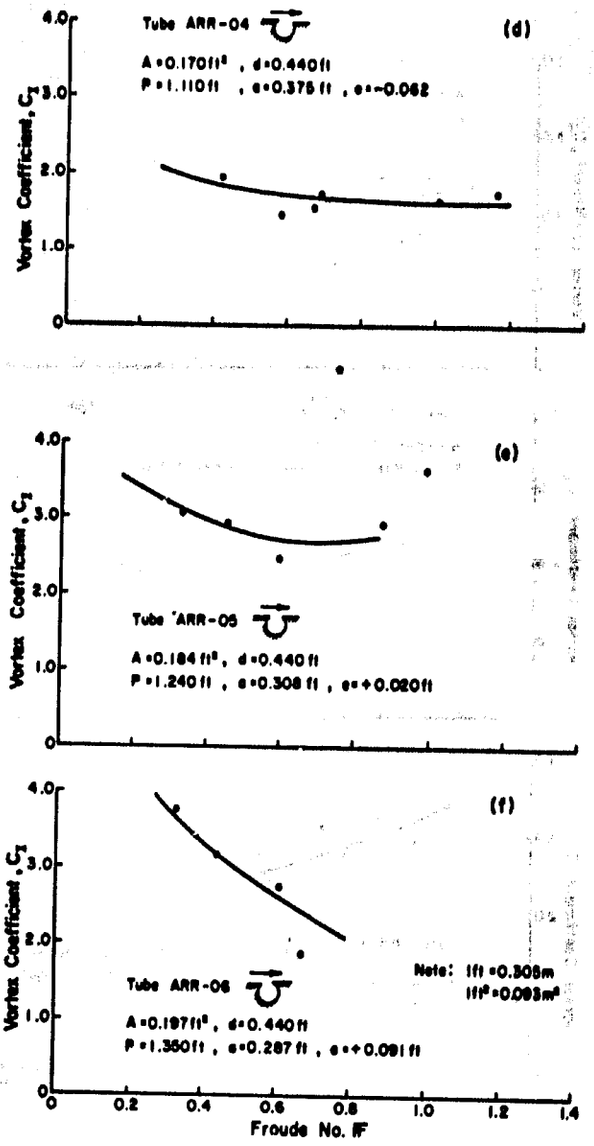

Figure 4(d) - 4(f). Variation of Vortex Coefficient C_I with Froude No. IF in Robinson's Vortex Tubes. In all Tubes, B = 8.0 ft and $\phi = 45°$.

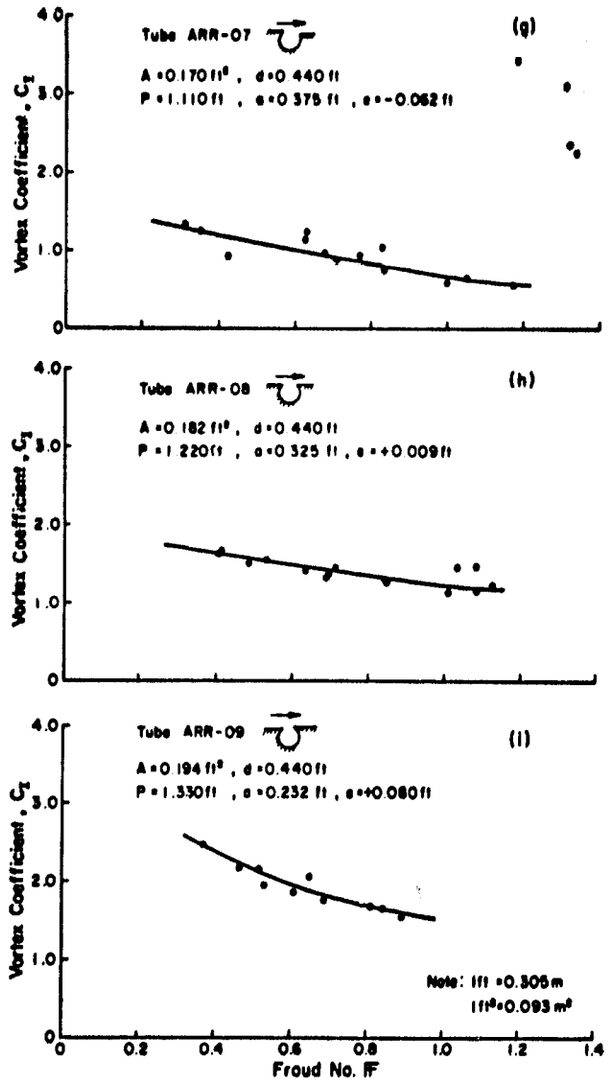

Figure 4(g) - 4(i). Variation of Vortex Coefficient C_I with Froude No. IF in Robinson's Vortex Tubes. In all Tubes, B = 8.0 ft and $\phi = 45°$.

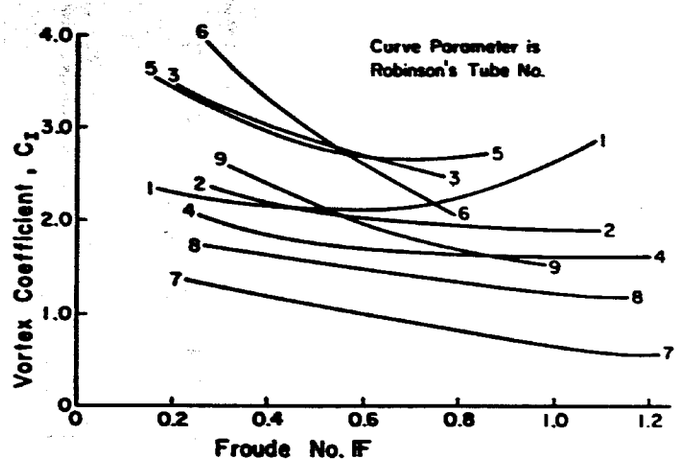

Tube No.	Shape	A, ft²	d, ft	a, ft	e, ft
ARR-01	⊔	0.244	0.417	0.625	−0.062
ARR-02	⊔	0.261	0.417	0.561	+0.005
ARR-03	⊔	0.280	0.417	0.520	+0.064
ARR-04	⊔	0.170	0.440	0.375	−0.062
ARR-05	⊔	0.184	0.440	0.308	+0.020
ARR-06	⊔	0.197	0.440	0.287	+0.091
ARR-07	⊔	0.170	0.440	0.375	−0.062
ARR-08	⊔	0.182	0.440	0.325	+0.009
ARR-09	⊔	0.194	0.440	0.232	+0.080

Note : 1 ft =0.305m
1 ft²=0.093m²

Figure 5. Average C_I - F Relations for Robinson's Vortex Tubes.

Variation of Hydraulic Quantities Along the Tube

As stated earlier, the flow model shows that all the hydraulic quantities relating to the vortex tube decay exponentially from the discharge end of the tube upwards. The implication of this exponential variation is that the discharge Q_T enters through a relatively small length of the tube close to the discharge end. To illustrate this point the variation of different hydraulic quantities pertaining to Robinson's run ARR-01-12 has been calculated. For this run, the data are:

$(H + \frac{d}{2}) = 0.528$ ft, $p_{c_e} = 0$, $F = 0.496$, $Q_T = 0.92$ cfs, $\phi = 45°$, $B = 8.0$ ft, $f = 0.016$, $C_v = 0.985$, $C_{1L} = 1.00$, $C_a = 0.60$ and $C_I = 2.621$. The corresponding values $A_* = 0.395$, $B_* = -1.720$, $C_* = -0.009$ and the largest real root of Equation (16) is $k = 1.125$.

The following dimensionless quantities are introduced to illustrate the variation of hydraulic parameters along the tube:

$$s_* = s/L$$

$$Q_* = Q(s)/Q_T \tag{25}$$

$$q_{I_*} = q_I(s)\ L/Q_T \tag{26}$$

$$\Delta h_* = \Delta h\ (s)/\ h(L) \tag{27}$$

and

$$\omega_* = \omega(s)/\omega(L)\ . \tag{28}$$

Figure 6 shows the variation of Q_*, q_{I_*}, Δh_* and ω_* along s_*. Also shown in these figures are the variation of the same parameters if C_I is reduced to half its value, 1.310. It is seen that:

1. The active length of the tube is about 0.4 times the total length.
2. A lower value of C_I increases the total discharge Q_T through the tube, but it decreases the effective length of the tube to 0.33 of the tube length.

It is concluded that the role of the vortex motion in the vortex tube is to increase the active length of the vortex tube for a given flow condition. This conclusion bears on the sediment conduction through the tube and is discussed later.

SEDIMENT INFLOW IN A VORTEX TUBE

The vortex tubes are generally built into bed contractions. The flow starts to develop new velocity and sediment concentration profiles at the bed contraction which are different from the profiles in the developed flow of the approach channel. In subcritical channel flow the depth constricts over the bed contraction thus providing a favorable pressure gradient. If the transition between the channel bed and the bed contraction is well rounded and gradual, the flow does not separate from the boundary. In such cases, it may be possible to compute the velocity and sediment concentration profiles approaching the vortex tube. However, if the flow does not undergo separation from

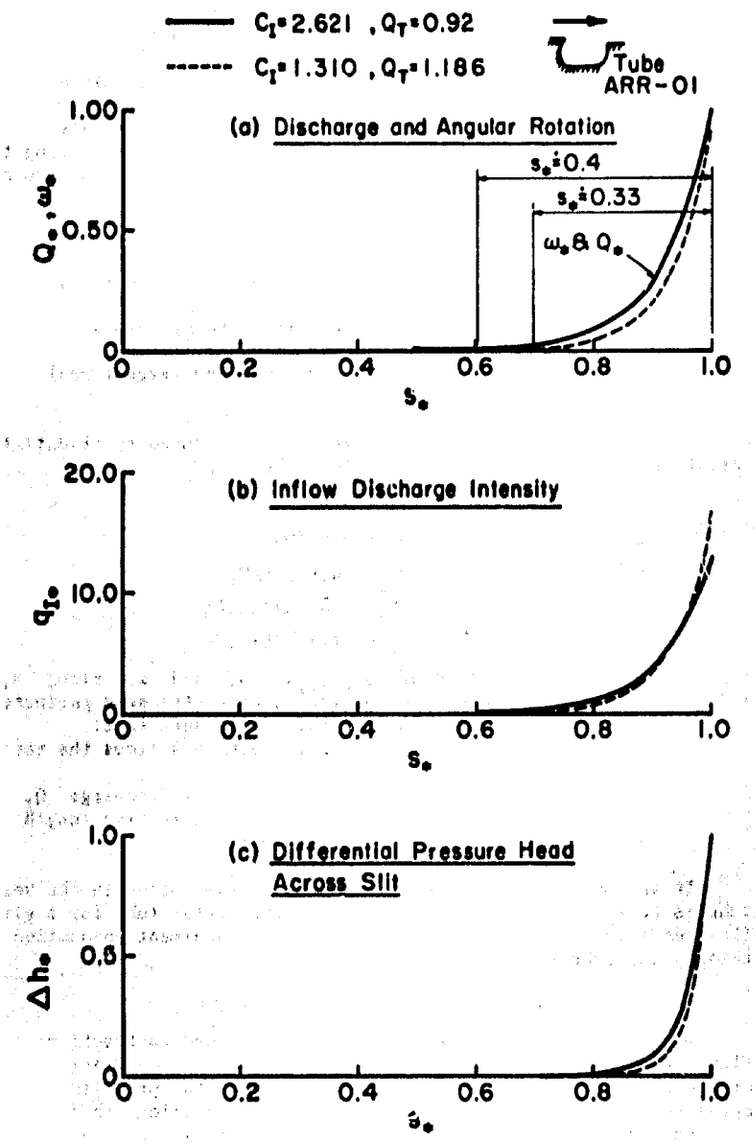

Figure 6. Calculated Variation of Dimensionless Flow Parameters Along Tube Length - Run ARR-01-12.

the solid boundary and the distance between the upstream edge of the contraction and the vortex tube is small--say less than about two flow depths depending on the bed material size and the amount of bed contraction--it is possible to make some simplifying assumptions. It is assumed herein that if the preceding conditions are satisfied, then the sediment concentration in each stream tube remains unchanged between the equilibrium channel flow and the flow approaching the vortex tube. With this assumption and with the use of the hydraulic solution of the tube flow, it is possible to determine the sediment conduction in a vortex tube. This approach requires an analytical model for the velocity and sediment distribution in the equilibrium channel flow. A number of such models are available but mostly they involve implicit functions requiring numerical and sometimes trial and error solutions. In the following development, an approximate two dimensional model of velocity and sediment distribution in sandbed channels (8) is used. This model uses explicit power relations for all the hydraulic and sedimentation quantities in terms of the depth of flow. Phenomenologically its structure is the same as the Einstein bedload function (4) and the writer's model (6) for flow in sandbed channels. The details of this model have been described elsewhere (8). The advantage of using this model in the context of the present problem is that one can calibrate the model when needed and the results are obtained in closed form.

Model for Flow in Sandbed Channels

Consider an equilibrium flow with a discharge intensity q on a sandbed with the median bed material size, D and a Froude number F_a (Fig. 1). Then the resistance function for the flow (8) in fps units is

$$n = k_1 D^a / F_a^b \tag{29}$$

$$n' = 0.0342\, D^{1/6} \tag{30}$$

and

$$H'_a = H_a \left(\frac{n'}{n}\right)^{3/2} \tag{31}$$

where n = Manning's roughness coefficient for the flow, k_1 = an empirical coefficient, a and b = empirical exponents, n' = grain-associated Manning's n for the flow, H_a = depth of equilibrium flow, $\rho g H'_a S = \rho U'^2_* =$ grain-associated boundary shear stress and S = energy gradient in the flow. In Equation (29), k_1, a and b are evaluated in the range of flow conditions experienced in the channel. In addition to Equations (29) to (31), the bed material transport and shear parameters, ϕ_* and Ψ_* are defined as:

$$\phi_* = g_b \left[\frac{1}{g(G-1)D^3}\right]^{1/2} \tag{32}$$

$$\Psi_* = (G-1)\frac{D}{H'_a S} \tag{33}$$

and

$$\phi_* = a_1 \Psi_*^{b_1} \tag{34}$$

where g_b = bed-load in solid volume per second per unit width of the channel, G = specific gravity of the bed material and a_1, b_1 are determined from Figure 9 of reference (4) for a range around Ψ_*. Alternately, a_1 and b_1 can also be determined from the available field data.

Suspended Load Distribution

The bed-load is assumed to move in bed layer of thickness 2D and the velocity of sediment in the bed layer is 11.6 U_*'. Thus the reference concentration of bed material, c_a, at the edge of the bed layer is

$$c_a = \frac{g_b}{(11.6\ U_*')(2D)} \tag{35}$$

where c_a is in units of solid volume per unit volume of space. The vertical distribution of bed material concentration is not very sensitive to the underlying assumption of the variation of sediment diffusion coefficient, ε_s (or the shear distribution) along the depth of flow. The major uncertainty in the computation of suspended load distribution comes from the selection of the Rouse number, z (6). For simplicity, it is assumed herein that the turbulent diffusivity ε_s varies linearly in the depth of flow as $\varepsilon_s = \kappa U_* y$, where κ = von Karman's constant, U_* = shear velocity and y = distance from the average sand bed. The resultant bed material concentration profile is

$$c_y = c_a \left(\frac{2D}{y}\right)^z \tag{36}$$

where $z = \frac{w}{\kappa U_*}$, and w = fall velocity of sediment size D.

The velocity distribution in the vertical is assumed to follow a power law

$$\frac{U_y}{U_*'} = a_2 \left(\frac{y}{D}\right)^{b_2} \tag{37}$$

where the exponent b_2 is selected herein as 1/6 and coefficient a_2 can be determined by equating the grain associated resistance factors from Equations (30) and (37).

The discharge q_y and bed material load g_y from the mean bed up to a distance y from the bed can be calculated as:

$$q_y = \int_0^y u_y\, dy \tag{38}$$

$$g_y = g_b + \int_{2D}^{y} c_y\, u_y\, dy\ . \tag{39}$$

For a specified discharge q_y, Equation (39) can be expressed as

$$g_y = \ell_1 H_a^{m_1} + \ell_2 H_a^{m_2} + (q_y)^{m_0}\, \ell_3 H_a^{m_3} \tag{40}$$

where y = the distance from channel bed up to which the discharge per unit width of the channel is q_y, g_y = total bed material load up to

y, $m_0 = (1 + b_2 - z)/(1 + b_2)$ and ℓ_1, ℓ_2, ℓ_3, m_1, m_2, m_3 are functions of the known bed material, channel flow and transport parameters earlier introduced in Equations (29) to (37). Equation (40) can be used to calculate the bed material inflow in the vortex tube corresponding to the inflow of a discharge intensity, q_y per unit length of the tube. Use of Equation (40) will be illustrated with a numerical example later.

WATER AND SEDIMENT CONDUCTION IN A VORTEX TUBE

The hydraulic and bed material inflow solutions for the vortex tube can be combined to yield the water and sediment conduction under specified conditions of channel flow.

Let a vortex tube with specified size, shape and C_I - IF characteristics be laid at an angle ϕ in a rectangular channel of width, B (Fig. 1). Let the bed contraction have an elevation Δz above the channel bed. The depth of flow over the vortex tube is given by

$$H + \frac{q^2}{2gH^2} = H_a + \frac{q^2}{2gH_a^2} - \Delta z \qquad (41)$$

To solve for the flow through the vortex tube, the analysis was based on coordinate s measured along the length of the tube. In the following development for the water and sediment conduction, it is more convenient to work in terms of x, the distance measured from the blind end of the vortex tube along a direction normal to the channel flow (see Fig. 1). Let q_{Ix} be the discharge inflow rate for the vortex tube per unit width of the channel at distance x (Fig. 2). From Equation (18),

$$q_{Ix} = Q_T\, k_* \exp\,[k_*(x-B)] \qquad (42)$$

where $k_* = k/\sin\phi$, x = distance measured normally to the channel axis from the blind end of the vortex tube and Q_T = total tube discharge at the outlet.

Combining Equations (42) and (40), the tube discharge and the bed material load inflow up to any distance x is

$$Q_*(x) = \int_0^x q_{Ix}\, dx \qquad (43)$$

and

$$G_*(x) = \int_0^x g_y\, dx \qquad (44)$$

There is a question about the lower limit of integration in Equation (44). Because the discharge within the tube varies exponentially it is understood that up to some distance x_0 from the blind end, the water discharge Q in the tube will not be enough to move the sediment inflow to the discharge end of the tube. The lower limit of integration in Equation (44) should therefore be replaced by x_0. It is assumed that for $0 \leq x \leq x_0$ the tube does not contribute to bed

material removal after the tube has been filled up in this reach by the falling bed load. To develop a criterion for x_0, it is further assumed that the incoming sediment load will be deposited in the tube as long as

$$\frac{V_r}{w} \leq 1 \tag{45}$$

where V_r = effective velocity in the tube = $\sqrt{(\frac{Q^2}{A}) + V_c^2}$ and w = fall velocity of sediment size D. With this criterion,

$$x_0 = \frac{-1}{k_*} \ln \left[\frac{Q_0}{wA} \left\{1 + \left(\frac{kA\, C_I \sin\phi}{C_a\, a}\right)^2\right\}^{1/2}\right] \tag{46}$$

where $Q_0 = Q_T \exp(-k_* B)$ and other terms have been defined earlier. The discharge $Q_*(B)$ at the end of the tube = Q_T and the bed material load

$$G_*(B) = \int_{x0}^{B} g_y(x)\, dx$$

$$= (\ell_1 H_a^{m_1} + \ell_2 H_a^{m_2})(B - x_0) + \ell_3 H_a^{m_3} \frac{k_*^{m_0} Q_T^{m_0}}{k_* m_0} \left[1 - e^{k_* m_0 (x_0 - B)}\right] \tag{47}$$

Equation (47) defines the total bed material load removed by the tube in solid volume per second. The bed material concentration in the extracted flow is

$$C_r = \frac{G G_*(B)}{Q_T} 10^6 \text{ ppm} \tag{48}$$

where G = specific gravity of the sediment. The use of this sediment conduction model is next illustrated for the vortex tube used in Robinson's series-8 (refer Table 1).

NUMERICAL EXAMPLES

The use of the preceding model of sediment and water conduction in vortex tubes is illustrated in the following for Robinson's tube No. 8 (ARR-08, Table 1). The dimensions of this tube are shown in Table 1. The C_I - F relationship for this tube is shown in Figure 4(h).

Three numerical examples are solved in Tables 2, 3 and 4. In the first example, the sediment extraction through the tube is studied for the variation of F_a in the channel flow while keeping the discharge end of the tube flowing free ($p_{ce} = 0$). In the second and third examples, the effect of varying $e_{\Delta z}$ and p_{ce} on the sediment ejection is studied. Similar investigations can be made to study the design aspects of a given vortex tube provided its C_I - F characteristics are known. The following data are given:

TABLE 2. CALCULATED VARIATION OF WATER AND SEDIMENT CONDUCTION IN VORTEX TUBE (ARR-08) FOR DIFFERENT VALUES OF FROUDE NUMBER, F_a (Δ_z = 0.10 ft).

	1	2	3	4	5
Channel:					
Froude number, F_a	0.30	0.40	0.50	0.57	0.58
Flow depth, H_a, ft	1.292	1.067	0.919	0.842	0.832
Energy gradient, S x 10^4	2.208	2.851	3.480	3.912	3.974
Shear Velocity, U_*, ft/sec	0.303	0.313	0.321	0.326	0.326
Grain-associated U_*' ft/sec	0.116	0.138	0.159	0.172	0.174
Bed load, g_b cfs/ft width x 10^4	1.386	3.609	6.265	8.401	8.744
Reference concentration, C_a, solid volume/unit volume x 10^2	2.906	6.350	9.614	1.190	1.225
Rouse number, z	1.824	1.766	1.723	1.698	1.694
Total Bed Material load, g_t, lb/sec/ft x 10^2	4.491	1.245	2.276	3.226	3.296
Concentration, ppm	288	798	1459	2068	2113
Vortex Tube:					
Flow depth, H, ft	1.180	0.943	0.770	0.645	0.623
Froude number, F	0.344	0.481	0.652	0.850	0.896
Coefficient C_I	1.697	1.587	1.454	1.308	1.280
Parameter A_1	9.726	9.223	8.662	8.103	8.001
Exponent k_e	1.342	1.371	1.407	1.445	1.452
Parameter A_2	0.996	1.034	1.083	1.139	1.151
Differential head at outfall, $\Delta h(L)$ ft	1.400	1.163	0.990	0.865	0.843
Tube discharge, Q_T, cfs	1.241	1.150	1.084	1.037	1.029
Distance, x_0, ft	5.164	5.297	5.428	5.552	5.574
Water and Sediment Discharge					
Discharge Q_T, cfs	1.241	1.150	1.084	1.037	1.029
Bed Material load, G_s lb/sec.	0.123	0.320	0.550	0.719	0.744
Concentration, ppm.	1584	4460	8129	11101	11583

Note: 1 ft = 0.305 m; 1 lb/sec/ft = 1.488 kg/sec/m

1 ft/sec = 0.305 m/sec; 1 cfs = 0.028 m^3/sec

1 cfs/ft = 0.093 m^3/sec/m; 1 lb/sec = 0.454 kg/sec

TABLE 3. CALCULATED VARIATION OF WATER AND SEDIMENT CONDUCTION IN VORTEX TUBE (ARR-08) FOR DIFFERENT BED CONTRACTION, Δz (F_a = 0.30).

	1	2	3	4	5
Channel:					
Same as in Case 1 Table 2					
Vortex Tube:					
Bed contraction, Δz ft	0.10	0.20	0.30	0.40	0.482
Flow depth, H ft	1.292	1.064	0.940	0.798	0.579
Froude number, F	0.344	0.401	0.483	0.618	1.000
Coefficient, C_I	1.697	1.648	1.584	1.479	1.230
Parameter, A_1	9.726	9.496	9.210	8.765	7.829
Exponent, k_*	1.342	1.355	1.372	1.400	1.465
Parameter, A_2	0.996	1.013	1.035	1.074	1.170
Differential head at outfall, $\Delta h(L)$ ft	1.400	1.284	1.160	1.018	0.799
Tube discharge Q_T cfs	1.241	1.197	1.149	1.094	1.010
Distance, x_0 ft	5.164	5.226	5.300	5.405	5.617
Water and Sediment Discharge:					
Discharge, Q_T cfs	1.241	1.197	1.149	1.094	1.010
Bed material load G_* lb/sec	0.123	0.121	0.117	0.112	0.103
Concentration, ppm	1584	1617	1630	1646	1640

Note: 1 ft = 0.305 m; 1 lb/sec/ft = 1.488 kg/sec/m
1 ft/sec = 0.305 m/sec; 1 cfs = 0.028 m^3/sec
1 cfs/ft = 0.093 m^3/sec/m; 1 lb/sec = 0.454 kg/sec

TABLE 4. CALCULATED VARIATION OF WATER AND SEDIMENT CONDUCTION IN VORTEX TUBE (ARR-08) FOR DIFFERENT VALUES OF WORKING HEAD AT THE DISCHARGE END $\Delta h(L)$ (BED CONTRACTION, $\Delta z = 0.10$ ft, $F_a = 0.30$).

	1	2	3	4	5	6	7
Channel:							
Same as in Case 1 Table 2							
Vortex Tube:							
Differential head, $\Delta h(L)$ ft	0.980	1.120	1.260	1.400	1.540	1.680	2.100
Distance, x_0 ft	5.297	5.247	5.203	5.164	5.128	5.096	5.013
All other quantities except Q_T remain unchanged							
Water and Sediment Discharge:							
Discharge, Q_T cfs	1.038	1.110	1.178	1.241	1.302	1.360	1.520
Bed material load, G_* lb/sec	0.117	0.119	0.121	.123	.124	.126	.130
Concentration, ppm	1803	1718	1646	1584	1530	1482	1371

Note: 1 ft = 0.305 m; 1 lb/sec/ft = 1.488 kg/sec/m
1 ft/sec = 0.305 m/sec; 1 cfs = 0.028 m^3/sec
1 cfs/ft = 0.093 m^3/sec/m; 1 lb/sec = 0.454 kg/sec

Approaching Channel Flow:

Q = 20.0 cfs (0.566 m^3/sec)

B = 8.0 ft (2.438 m)

D = D_{50} = 0.54 mm = 0.00177 ft

w = 0.221 ft/sec (0.067 m/sec)

$k_1 D^a$ = 0.0192

b = 0.666

IF_a = varies

Vortex Tube

Δz = 0.10 ft (0.030 m)

ϕ = 45°

Table 2 shows the variation of hydraulic and sediment transport parameters as IF_a is varied from 0.30 to 0.58. The bed material concentration in the discharge extracted through the vortex tube calculated in this table is plotted in Figure 7 against IF. Robinson's data for series 8 is also plotted on this figure. It is seen that for $IF \leq 1$, the results of analytical model lie close to his data. Note that the total discharge in Robinson's data used in Figure 7, varies from Q = 16.40 to 21.39 cfs (1.53 to 1.99 m^3/sec). The correspondence between the results of the analytical model and the laboratory measurement seen in Figure 7 is very encouraging. Note that the hydraulic model for flow has been verified from the gross measurements of the tube flow (Figure 4(h)) and Einstein's bed-load function (4) has been used for sediment transport quantities.

Another example of the use of this model is illustrated in Table 3. In this example, the channel flow is the same as in case 1 of Table 2 but the bed contraction, Δz is varied and the consequent change in sediment conduction through the tube is studied. This table shows that as Δz is increased from 0.100 to 0.482 ft. (0.031 to 0.147 m), the bed material concentration remains almost unaltered, while the discharge Q_T decreases by about 19 percent.

The third example is the study of the effect of differential head $\Delta h(L)$ at the discharge end of the vortex tube on the water and sediment conduction through the tube. In the previous two examples it was assumed that the tube is discharging freely, so that the centerline pressure at the discharge end $p_{ce} = 0$. In the present example, it is assumed that $\Delta h(L)$ can be decreased by submergence of the discharge end or increased by passing the tube discharge through a conduit and discharging it at a lower level. The basic data in this example also pertain to case 1 of Table 2.

The results in Table 4 show that an increasing $\Delta h(L)$, also increases the discharge, Q_T and the total sediment load, $G_*(B)$. However, the bed material concentration in the tube discharge decreases. This result can be explained by the fact, that by increasing $\Delta h(L)$ the distance y from which the discharge is withdrawn in

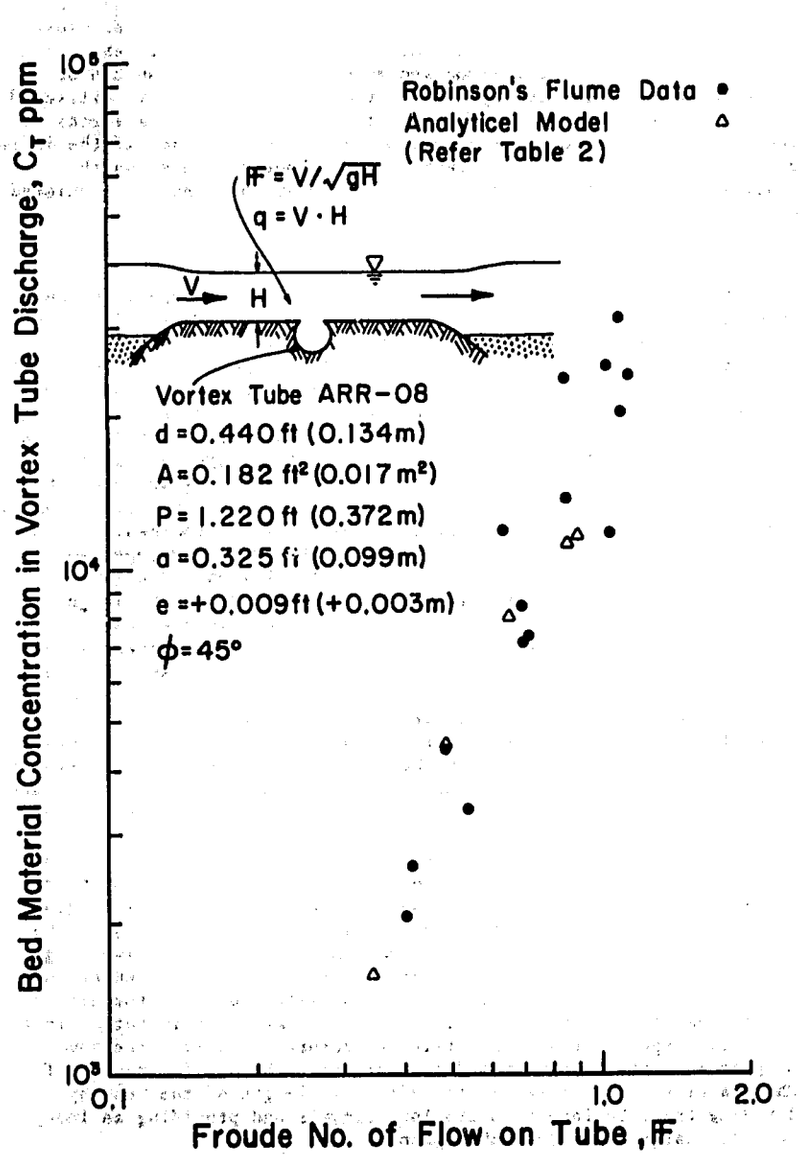

Figure 7. Variation of Bed Material Concentration in Vortex Tube Discharge, Robinson's Tube ARR-08.

the tube, is increased throughout the active length $(B - x_0)/\sin\phi$ of the tube and the average sediment concentration in a layer close to the bed decreases as the thickness of this layer increases. It can be stated here that the maximum bed material concentration can be extracted with a sediment ejector if the bed-layer alone is extracted from the total width of the flow and for a given Q_T in a vortex tube, the maximum bed material extraction can be obtained if the inflow discharge intensity q_I is constant throughout the tube length. Analysis shows that this ideal inflow distribution cannot be achieved with a prismatic tube.

CONCLUSION

The continuous flow sediment removal structures depend on the unequal distribution of sediment concentration in a flow. In these structures a portion of the flow is extracted from the region containing the higher concentration. In fully developed two dimensional flows in straight sandbed channels, the largest concentration occurs in the bed layer and decreases rapidly towards the surface resulting in a skewed concentration profile. Also the difference in concentration from the bed to the surface is greater for larger particles (larger z) than for smaller particles (smaller z). Therefore, in two dimensional fully developed flows, a larger bed material concentration can be removed for the coarser sizes and for withdrawals close to the bed. It is important that the flow be fully developed so the skewed concentration profile exists. If the skewness of a fully developed concentration profile has been disturbed, say by large scale turbulence, this principle cannot be used. In the case of three dimensional channel flow, as in bends, there is a skewness of sediment concentration along the depth of flow as well as along the width of the channel. This leads to an even greater facility in sediment removal because the concentration is higher on the inner side of the bend than under corresponding conditions in two dimensional flow. Another consideration in the design of sediment removal systems is that the sediment removed should also be conveyed out of the system. Otherwise, the removal structure can become inoperative due to clogging.

The vortex tube sediment ejector is basically designed for two dimensional flows. However as the analysis presented herein shows, a prismatic vortex tube does not draw uniformly through its length. In fact, under most operating conditions, a prismatic circular tube with $a \doteq d/4$, and $Q_T \doteq 0.5\ Q/B$ may only have an effective length of the tube equal to about 6d. For this reason any arrangement that can increase the channel bed material concentration near the discharge end of the vortex tube will increase the sediment concentration in the tube discharge. Parshall's riffle-deflectors (9) served the same purpose in a predominantly bed load stream. Ahmad's (2) design of D.G. Khan Canal ejector increases the effective length of the tube by dividing the tube length in smaller segments and providing an independent discharge tube for each segment.

Of necessity, the sediment ejectors are placed in reaches with unstable bed conditions. Due to the seasonal nature of most excess sediment loads, the bed elevation and the bed forms in the approach channel may vary in time within wide limits. A vortex tube located

in dune bed may get buried and become inoperative. Bed contractions help if the bed form on the contraction is flat bed.

An analytical model of the flow and sediment conduction through a vortex tube has been developed herein. This model combines the spatially varied flow equations with the sediment transport model in sand bed channels. The empirical coefficients introduced in the model have been investigated with the help of Robinson's 8-ft flume data (10). It is found that the coefficients of velocity C_v, of area C_a and of lateral momentum inflow C_{IL} can be considered as constants for the tubes investigated by Robinson. However, the vortex flow coefficient, C_I is found to be a function of the tube geometry and the Froude number of flow on the tube. Knowing the C_I - IF relation for a specific tube geometry, it is possible to use this model to investigate various characteristics of the vortex tube flow. Three numerical examples have been used to show the verification of laboratory study data, and the effect of variation of parameters on the sediment conduction through the tube.

The analysis reported herein is restricted to a limiting Froude number of 1 on the bed constriction, which is the range applicable to most sand bed channels.

ACKNOWLEDGEMENTS

The writer wishes to express his thanks to A. R. Robinson for making available his original experimental records and data. The study reported herein is part of a continuing research on the Alluvial River Mechanics Project, supported by National Science Foundation Grant No. ENG72-00274 A01. It was also partly supported by US AID grant No. AID/csd-2460 on Optimum Utilization of Water Resources to Colorado State University. The future plans on this study include field investigations on prototype vortex tubes in sand bed canals in Pakistan under National Science Foundation Special Foreign Currency Grant No. OIP73-002277 A01 to Water and Power Development Authority, Pakistan on the project: "A Study of Alluvial River Mechanics on Link Canals."

APPENDIX I. - REFERENCES

1. Ahmad, M., "Final Recommendations from Experiments on Silt Ejector of D. G. Khan Canal," Hydraulic Research, IAHR, 1958.

2. Ahmad, M., "Vortex Tube Sand Trap," Discussion, "Vortex Tube Sand Traps," by A. R. Robinson, Transactions, ASCE, Vol. 127, Pt. III, 1962.

3. Brown, D.R.M., "A Study of the Factors Influencing the Efficiency of Vortex Tube Sand Traps," Proceedings, Institute of Civil Engineers (London), June 1964.

4. Einstein, H.A., "The Bed-Load Function for Sediment Transportation in Open Channel Flow," Technical Bulletin 1026, U.S.D.A., Soil Conservation Service, 1950.

5. Koonsman, G.L., "Efficiency of a Vortex Tube Sand Trap," M.S. Thesis, Colorado State University, Fort Collins, Colorado, 1950.

6. Mahmood, K., "FLow in Sand-Bed Channels," Cususwash Water Management Technical Report No. 11, Colorado State University, Fort Collins, Colorado, 1971.

7. Mahmood, K., "Sediment Routing in Irrigation Canal Systems," Journal of Irrigation and Drainage Division, ASCE, Vol. 100 No. IR1, 1974.

8. Mahmood, K., "Mathematical Modeling of Morphological Transients in Sandbed Canals," Proceedings, XVIth Congress, IAHR, Sao Paulo, Brazil, 1975.

9. Parshall, R.L., "Model and Prototype Studies of Sand Traps," Transactions, ASCE, Vol. 117, 1952.

10. Robinson, A.R., "Vortex Tube Sand Trap," Transaction ASCE Vol. 127, Pt. III, 1962.

11. Rohwer, C., Code, W.E., and Brooks, L.R., "Vortex Tube Sand Trap Tests for 1933," Progress Report, U.S. Department of Agriculture, Bureau of Agricultural Engineering, Fort Collins, Colorado, 1934.